Pergamon

Int. J. Heat Mass Transfer. Vol. 41, No. 13, pp. 2013–2024, 1998

Printed in Great Britain
0017-9310/98 $19.00+0.00

PII: S0017-9310(97)00259-7

Thermal resistance of two solids in contact through a cylindrical joint

KEK-KIONG TIO† and KOK CHUAN TOH

School of Mechanical and Production Engineering, Nanyang Technological University, Singapore 639798, Republic of Singapore

(*Received* 26 *November* 1996 *and in final form* 13 *August* 1997)

Abstract—The steady-state heat-conduction problem of two semi-infinite solids in contact through a cylindrical joint is, by physical symmetry and uniqueness of solution, reduced to the problem of a cylinder of isothermal top surface in contact at its bottom with a semi-infinite solid. An analysis is carried out to investigate the thermal resistance of the system, taking into account the aspect ratio of the cylinder and the thermal conductivity of the solids. The effect of these parameters on the thermal resistance, which consists of the constriction resistance at the interface and the material resistance of the cylinder, is examined and discussed. © 1998 Elsevier Science Ltd. All rights reserved.

1. INTRODUCTION

It is well known that when two nominally flat solid surfaces are brought into contact, the actual contact takes place over a fraction of the interface only. At the interfacial regions where contact does not exist, air may be present. However, the heat flow across the air gaps is negligible due to the very low thermal conductivity of air. Consequently, the heat conducted from the warmer solid to the cooler one is constricted to flow through the contacting regions only. The constriction of heat flow then results in the "thermal constriction resistance" at the interface.

The study of thermal constriction resistance dates back several decades [1], and reviews on this subject are available [2–5]. In general, we can identify two schools of approach to the problem of contact heat transfer. In the first one, the thermal problem of contact conductance is, to a varying degree, coupled with the mechanical problem of two solids in contact. The constriction resistance is then determined as a function of contact pressure, the mechanical properties of the solids, and surface topography. Examples of this school include, but by no means are limited to, the works of Cooper *et al.* [6], Sayles and Thomas [7], Bush and Gibson [8], and a more recent study by Majumdar and Tien [9], who employ the concept of fractals to characterize the surface topography of the solids. The second school of approach to the problem of contact conductance is to decouple the thermal and mechanical problems. In this approach, the contact geometry is assumed to be known and fixed, and the problem involves thermal calculations only. For a reasonably simple contact geometry, detailed calculations of temperature and heat flow can usually be carried out. In this paper, we shall take up the second approach.

In the second school of approach to the problem of thermal constriction resistance, several authors, such as Hunter and Williams [10], Gibson [11], and Negus and Yovanovich [12], have modeled the problem with an isothermal contact area on the top surface of an infinitely long circular cylinder of adiabatic lateral surface. The case of a cylinder of finite length has also been treated by Faltin [13] and Gladwell and Lemczyk [14], whose analysis covers a broad spectrum of boundary conditions. Another popular model is the problem of multiple contact areas on the surface of a semi-infinite solid. In this regard, Greenwood [15] has considered the case of a single cluster of circular contacts, while Beck [16] has treated the case of regularly arranged circular contacts heated by a uniform heat flux. In a more recent study, Tio and Sadhal [17] have also treated the problem of a periodic array of isothermal contacts, in addition to contact areas heated by a uniform heat flux. While the works cited above all involve discrete contact areas, the problem of a multiply connected contact region has also been studied. Tio and Sadhal [18] have modeled this problem with discrete circular gaps, i.e., regions of no contact, arranged periodically on the otherwise isothermal surface of a semi-infinite solid. A two-dimensional problem in which two solids are in partial contact at their interface due to the presence of interstitial materials has also been considered [19, 20].

In this paper, we shall consider a problem which, in some respect, is a generalization of the work of Tio and Sadhal [17]. Specifically, we shall consider the problem associated with two solids in contact through a cylindrical joint of finite length, as opposed to the circular disks of zero thickness studied by Tio and Sadhal [17]. Our main objective is to investigate how

† Author to whom correspondence should be addressed.

NOMENCLATURE

a_n coefficients in the series expansion (19)
b_n coefficients in the series expansion (25)
b_0 (N) b_0 obtained using the first N equations (30)
C_{nm} equation (32)
F_m equation (28)
G_m equation (29)
$h = H/R$ dimensionless height of the cylinder
h_α, h_β, h_ϕ metric coefficients, equations (23), (24)
H height of the cylinder, Fig. 2
$i = \sqrt{-1}$ imaginary unit
J_ν Bessel function of the first kind of order ν
k thermal conductivity
N number of equations (30) used in the calculation of b_n
P_n Legendre polynomial of degree n
Q_n, Q_n' Legendre function of the second kind of degree n, derivative of Q_n
$\dot{Q}$ rate of heat flow from the cylinder to solid 2
R radius of the cylinder
$\mathscr{R}$ thermal resistance, equation (11)
$\mathscr{R}_{tot}$ thermal resistance between solids 2 and 3
T temperature
T_0 temperature of the cylinder's top surface, Fig. 2
T_∞ far-field temperature.

Greek symbols
δ equation (36)
δ_{mn} Kronecker delta, equation (31)
ΔT difference between T_0 and the average surface temperature of solid 2
$\Delta T_{cylinder}$ difference between T_0 and the average temperature of the cylinder's bottom surface
ΔT_{if} difference between the average temperatures of the bottom surface of the cylinder and the entire surface of solid 2
ΔT_{tot} difference between the average surface temperatures of solids 3 and 2
ε equation (37)
Θ dimensionless temperature, equation (2)
λ_n nth positive root of J_1
μ conductivity ratio, equation (18)
φ dimensionless resistance, equation (17)
ψ dimensionless resistance, equation (16).

Subscripts
1 of solid 1 (the cylinder)
2 of solid 2
c constriction resistance
m material resistance.

Coordinate systems
(r, ϕ, z) cylindrical coordinates
(ϱ, ϕ, ζ) dimensionless cylindrical coordinates, equation (1)
(α, β, ϕ) oblate spheroidal coordinates.

the finite thickness of the cylinder, through its physical configuration and the thermal properties of its material, affects the thermal resistance.

Another motivation for the present study has its origin in the micro-electronics industry. In recent years, ball grid arrays (BGAs) have been suggested as the solution for future high performance electronic packaging because they can provide the much needed space saving and meet the increasingly stringent requirements of fine interconnection pitch. Consequently, a dense routing inside the printed circuit board and short electric paths between device components are then possible. For a brief review of BGA, we refer to the articles by Lau [21] and Romenesko [22]. Although package level BGA assemblies have been reported to have thermal performances as good as or even better than other packaging technologies, there has not been any comprehensive study of the thermal performance limits of BGA components. However, it is apparent that their heat dissipation characteristics depend critically on the joint conductance between the two boards connected by the BGA. In this paper, we shall analyze the solder joint as a cylinder between two semi-infinite solids. This analytical model is applicable to the SCC (Solder Column Connect) and, as a first approximation, the OMPAC (Over Molded Pad Array Carrier) and SBC (Solder Ball Connect) connection modes discussed by Adams [23].

As the name implies, a BGA system consists of an array of solder joints connecting two component boards. Therefore, a complete analysis of the heat transfer from one board to the other, via the solder joints, must take into account the thermal interactions of these joints. Even though analytical techniques to handle this type of problem exist [18, 24, 25], the

solution method for our problem may become much more difficult due to the more complicated geometry of the present study. For the sake of simplicity, so that we can analyze the problem and extract valuable information from it, we shall therefore ignore the thermal interactions of the solder joints. This is justifiable if the joints are sufficiently far apart from each other.

Our problem, then, is to analyze the heat transfer associated with a system comprising two solids, which we model to be semi-infinite, in contact through a cylindrical joint, as depicted in Fig. 1. At the interface between the cylinder and each of solids 2 and 3, perfect thermal contact is assumed. Since the temperature range of interests to us is sufficiently low so that radiative effects are not significant, we shall ignore this mode of heat transfer. Furthermore, we also assume that the heat transfer across the gap between solids 2 and 3 is negligible, on the ground that the fluid medium, usually air, filling the gap has a thermal conductivity which is much smaller than that of the solids. Therefore, we model the lateral surface of the cylinder and those of solids 2 and 3 not in contact with it to be impervious to heat flow. Finally, we shall be interested in steady-state heat transfer only. Thus, our problem consists of the analysis of the steady-state heat conduction from solid 3, which we assume to be the warmest, through the cylinder, and into solid 2. Of main interest to us will be the calculation of the thermal resistance associated with this system.

In general, the two semi-infinite solids must be assumed to have different thermal conductivities. However, for the sake of simplicity, we are interested only in the case in which the two solids have the same thermal conductivity. In this situation, we can follow Cooper *et al.* [6], and invoke the argument of geometrical symmetry and the uniqueness of solution, apart from an additive constant, to show that the temperature is uniform at the cross section of the cylinder midway between the two semi-infinite solids. Consequently, our original problem reduces to the heat transfer analysis in the simpler system depicted in Fig. 2. In the following developments, we shall be concerned with this simpler problem only.

2. PROBLEM FORMULATION

Introducing the dimensionless variables

$$\varrho = \frac{r}{R}, \quad \xi = \frac{z}{R} \tag{1}$$

$$\Theta_1 = \frac{T_1 - T_\infty}{T_0 - T_\infty}, \quad \Theta_2 = \frac{T_2 - T_\infty}{T_0 - T_\infty} \tag{2}$$

we shall now state the governing equations together with the boundary conditions. In solid 1, the steady-state temperature satisfies Laplace's equation

$$\nabla^2 \Theta_1 = 0 \tag{3}$$

and the boundary condition of

$$\xi = -h: \ \Theta_1 = 1 \tag{4}$$

$$\varrho = 1: \ \frac{\partial \Theta_1}{\partial \varrho} = 0 \tag{5}$$

where h is the dimensionless height of the cylinder. The temperature field in solid 2 is also governed by Laplace's equation

$$\nabla^2 \Theta_2 = 0 \tag{6}$$

and the boundary conditions of

$$\xi = 0, \quad \varrho > 1: \ \frac{\partial \Theta_2}{\partial \xi} = 0 \tag{7}$$

$$(\varrho^2 + \xi^2)^{1/2} \to \infty: \ \Theta_2 = 0. \tag{8}$$

Since the two solids are assumed to be in perfect thermal contact at their interface, the conditions of continuity of temperature and heat flux apply:

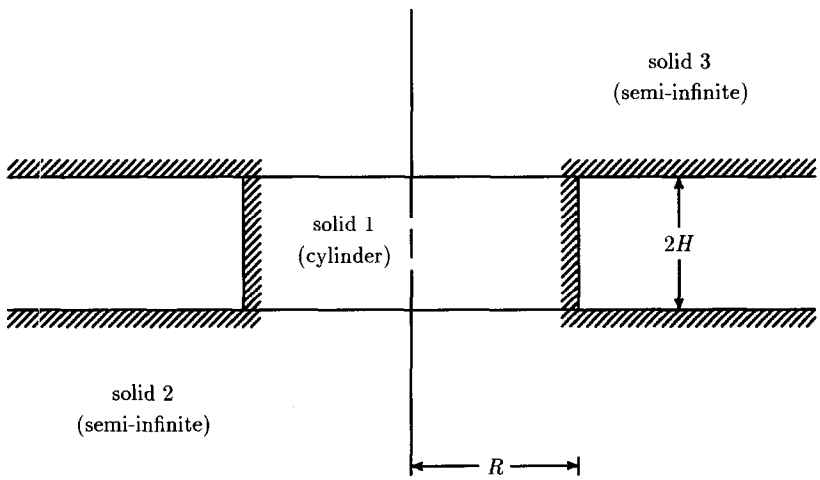

Fig. 1. Two semi-infinite solids in thermal contact through a circular cylinder.

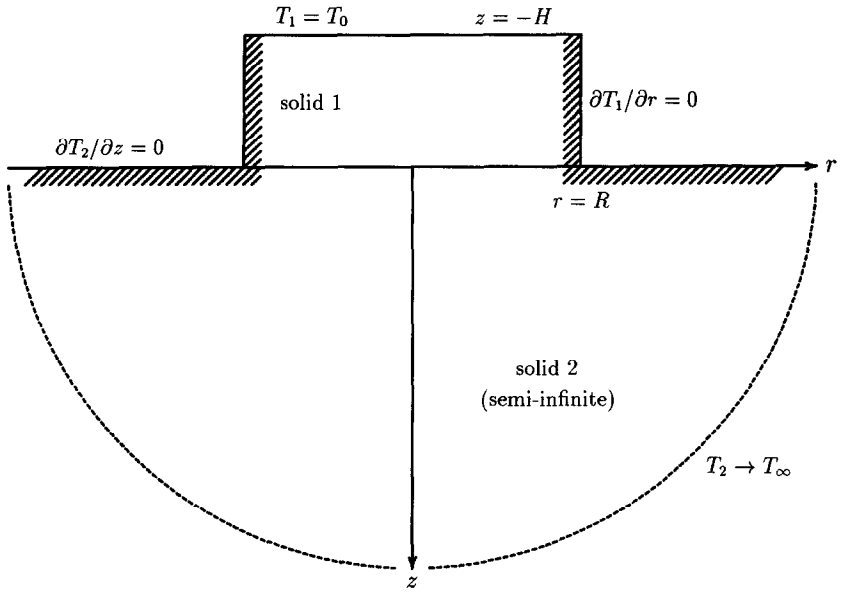

Fig. 2. Schematic diagram of the problem studied in this paper.

$$\Theta_1 = \Theta_2 \tag{9}$$

$$k_1 \frac{\partial \Theta_1}{\partial \xi} = k_2 \frac{\partial \Theta_2}{\partial \xi}. \tag{10}$$

In equation (10), k_1 and k_2 are the thermal conductivities of solids 1 and 2, respectively.

The main objective of this paper is to calculate the thermal resistance $\mathscr{R}$ and to investigate its behavior as a function of the parameters h, k_1, and k_2. Here, we define the thermal resistance as

$$\mathscr{R} = \frac{\Delta T}{\dot{Q}} \tag{11}$$

where $\dot{Q}$ is the rate of heat flow from the cylinder to the semi-infinite solid, and ΔT is the difference between the temperature of the isothermal surface of the cylinder and the average surface temperature of the semi-infinite solid. Obviously,

$$\Delta T = \Delta T_{\text{cylinder}} + \Delta T_{\text{if}} \tag{12}$$

where $\Delta T_{\text{cylinder}}$ is the axial temperature drop of the cylinder and ΔT_{if} is the difference between the average temperatures of the bottom of the cylinder and the entire surface of the semi-infinite solid. Thus, we can rewrite equation (11) as

$$\mathscr{R} = \mathscr{R}_{\text{m}} + \mathscr{R}_{\text{c}} \tag{13}$$

where $\mathscr{R}_{\text{m}}$ and $\mathscr{R}_{\text{c}}$ are the resistance due to the material of the cylinder and the constriction resistance at the interface of the two solids, respectively, and are given by

$$\mathscr{R}_{\text{m}} = \frac{\Delta T_{\text{cylinder}}}{\dot{Q}} \tag{14}$$

$$\mathscr{R}_{\text{c}} = \frac{\Delta T_{\text{if}}}{\dot{Q}}. \tag{15}$$

In this paper, we shall mainly be interested in $\mathscr{R}$ only, instead of its separate components. To facilitate our study of the thermal resistance, we introduce the dimensionless resistance ψ, which is defined as

$$\psi \equiv 4k_2 R\mathscr{R}. \tag{16}$$

In selecting the factor of $4k_2R$ to non-dimensionalize the thermal resistance $\mathscr{R}$, we have in mind the limiting case of $h = 0$. For this special case of an isothermal disk on an otherwise insulated surface of a semi-infinite solid, $\psi = 1$ (see, for example, the article of Tio and Sadhal [17]). Obviously, it is convenient to use equation (16) to investigate the behavior of $\mathscr{R}$ as we vary k_1 while holding k_2 fixed. In the opposite situation, in which we vary k_2 but keep k_1 fixed, it is more convenient to study the dimensionless resistance φ, which is given by

$$\varphi \equiv 4k_1 R\mathscr{R} = \frac{\psi}{\mu} \tag{17}$$

where

$$\mu = \frac{k_2}{k_1}. \tag{18}$$

In the next section, we shall solve the problem given by equations (3)–(10), and derive the formulas for ψ and φ.

3. SOLUTION

By employing the technique of separation of variables in the cylindrical coordinates (ϱ, ξ), we obtain the dimensionless temperature Θ_1 as

$$\Theta_1 = 1 + a_0(h+\xi) + \sum_{n=1}^{\infty} a_n \sinh \lambda_n (h+\xi) J_0(\lambda_n \varrho) \tag{19}$$

where J_0 is the Bessel function of the first kind of order zero, and λ_n are the positive roots of the Bessel function of the first kind of order one, i.e.,

$$J_1(\lambda_n) = 0. \tag{20}$$

The temperature Θ_1 as given in equation (19) satisfies the boundary conditions (4)–(5), irrespective of the coefficients a_n, which will be determined later.

To obtain the temperature field Θ_2, we first introduce the oblate spheroidal coordinates (α, β, ϕ), which are related to the cylindrical coordinates (r, ϕ, z) through the formulas

$$r = R \cosh \alpha \sin \beta \tag{21}$$

$$z = R \sinh \alpha \cos \beta. \tag{22}$$

The metric coefficients are given by

$$h_\alpha = h_\beta = R(\cosh^2 \alpha - \sin^2 \beta)^{1/2} \tag{23}$$

$$h_\phi = R \cosh \alpha \sin \beta. \tag{24}$$

In the oblate spheroidal coordinate system, the interface between solids 1 and 2 corresponds to $\alpha = 0$, while the surface of solid 2 not in contact with solid 1 is given by $\beta = \pi/2$. The positive z-axis corresponds to $\beta = 0$, and the far field (i.e., $(r^2+z^2)^{1/2} \to \infty$) is identified by $\alpha \to \infty$. By separation of variables [26], we obtain the temperature Θ_2 as

$$\Theta_2 = \sum_{n=0,2,\ldots}^{\infty} i b_n Q_n(i \sinh \alpha) P_n(\cos \beta) \tag{25}$$

where P_n is the Legendre polynomial of degree n, Q_n the Legendre function of the second kind of degree n, and $i^2 = -1$. Since $Q_n(i \sinh \alpha)$ is imaginary for zero and even n, we include the number i in equation (25) so that the coefficients b_n are always real. The temperature field Θ_2 as given by equation (25) satisfies the boundary conditions (7), (8).

To determine the coefficients a_n and b_n, we make use of the interface conditions (9), (10). From the condition of continuity of temperature, we obtain

$$a_0 = -\frac{1}{h} + 2\frac{1}{h} \sum_{m=0,2,\ldots}^{\infty} i b_m Q_m(i0) F_m(0) \tag{26a}$$

$$a_n = \frac{2}{\sinh(\lambda_n h)[J_0(\lambda_n)]^2} \sum_{m=0,2,\ldots}^{\infty} i b_m Q_m(i0) F_m(\lambda_n), \quad n = 1, 2, \ldots. \tag{26b}$$

Applying the condition of continuity of heat flux, we obtain

$$a_0 = -2\mu \sum_{m=0,2,\ldots}^{\infty} b_m Q'_m(i0) G_m(0) \tag{27a}$$

$$a_n = -\frac{2\mu}{\lambda_n \cosh(\lambda_n h)[J_0(\lambda_n)]^2} \sum_{m=0,2,\ldots}^{\infty} b_m Q'_m(i0) G_m(\lambda_n), \quad n = 1, 2, \ldots. \tag{27b}$$

The functions $F_m(x)$ and $G_m(x)$ are defined as follows:

$$F_m(x) = \int_0^1 u P_m([1-u^2]^{1/2}) J_0(xu)\, du \tag{28}$$

$$G_m(x) = \int_0^1 u[1-u^2]^{-1/2} P_m([1-u^2]^{1/2}) J_0(xu)\, du. \tag{29}$$

A discussion on the computation of the functions F_m and G_m will be given in the Appendix.

From the interface conditions (9), (10), we have obtained two sets of equations (26a), (26b) and (27a), (27b) for the two sets of unknown coefficients a_n and b_n. In principle, then, we can solve the two sets of equations for the unknown coefficients. Eliminating a_n from equations (26a)–(27b), we obtain an infinite set of simultaneous linear equations for the unknown b_m:

$$\sum_{m=0,2,\ldots}^{\infty} C_{nm} b_m = \frac{1}{2}\delta_{n0}, \quad n = 0, 1, 2, \ldots. \tag{30}$$

The Kronecker delta symbol δ_{mn} is defined by

$$\delta_{mn} = \begin{cases} 0 & \text{if } m \neq n \\ 1 & \text{if } m = n \end{cases} \tag{31}$$

and the coefficients C_{nm} by

$$C_{nm} = iQ_m(i0)F_m(\lambda_n) + \frac{\mu \tanh(\lambda_n h)}{\lambda_n} Q'_m(i0) G_m(\lambda_n) \tag{32}$$

where $\lambda_0 = 0$, λ_1, $\lambda_2, \ldots$ are the non-negative roots of the Bessel function J_1. In the next section, we shall discuss the results obtained by truncating the infinite set of equations given by (30) and solving the resulting finite set numerically. To solve this finite set of simultaneous linear equations, we shall use the Gauss–Jordan elimination scheme.

Of main interest in this paper is the calculation of the dimensionless resistances ψ and φ. However, we need to calculate first the rate of heat transfer $\dot{Q}$ from solid 1 to solid 2. To obtain $\dot{Q}$, we integrate the heat flux across the interface over the entire interfacial area:

$$\dot{Q} = -2\pi k_2 (T_0 - T_\infty) \int_0^{\pi/2} [h_\beta h_\phi]_{\alpha=0} \left[\frac{1}{h_\alpha}\frac{\partial \Theta_2}{\partial \alpha}\right]_{\alpha=0} d\beta = 2\pi b_0 R k_2 (T_0 - T_\infty). \tag{33}$$

Substituting the formula for $\dot{Q}$ given above into equation (11), and noting that the average surface temperature of solid 2 is equal to T_∞, we then obtain the dimensionless resistances as

$$\psi = \frac{2}{\pi b_0} \tag{34}$$

$$\varphi = \frac{2}{\pi \mu b_0}. \tag{35}$$

4. RESULTS AND DISCUSSION

Since equation (30) is an infinite set of simultaneous linear equations, we need to truncate it so that we can solve the resulting finite set of N equations for the N unknown coefficients b_m. However, before we can numerically extract any information from equation (30), we need to establish first the smallest acceptable value of N. In Fig. 3, we plot the quantity δ, which is defined by

$$\delta = \frac{b_0(1) - b_0(N)}{b_0(1)} \times 100 \tag{36}$$

as a function of N for the case of $\mu = 1.0$ and $h = 1.0$. In equation (36), $b_0(N)$ is the value of b_0 computed using the first N equations of the system of (30). From Fig. 3, we see that $b_0(N)$ has started approaching asymptotically the true value of b_0, which is equal to $b_0(N \to \infty)$, by the time we increase N to 20. Based on Fig. 3, we decide that it is sufficient to use the first 20 equations of the system of (30) to calculate b_0, which is the only unknown we need in the calculation of the dimensionless resistances [see equations (34), (35)].

To confirm that it is sufficient to use the first 20 equations of the system of (30), let us examine the quantity ε, which is defined as

$$\varepsilon = \frac{b_0(19) - b_0(20)}{b_0(19)} \times 10^6. \tag{37}$$

In Fig. 4, we plot the quantity ε versus the conductivity ratio μ with h being the parameter. It is seen that for a given h, ε decreases when a sufficiently small μ decreases or when a sufficiently large μ increases; furthermore, $\varepsilon \to 0$ as $\mu \to 0$ or $\mu \to \infty$. This is so because we can solve the system of (30) exactly for b_0 in these special cases of $\mu = 0$ and $\mu \to \infty$. From Fig. 4, we also observe that for a fixed μ (and a sufficiently large h), ε increases with a decreasing h. However, when h has decreased to a certain value, a further decrease in h results in the decrease of ε, as is evident from Fig. 5, which shows that $\varepsilon = 0$ when $h = 0$. In fact, for the special cases of $h = 0$ $h \to \infty$, we can solve the system of (30) exactly for b_0. Even though we present in Fig. 5 the results for $\mu = 0.5$, 1.0, 2.0 only, our calculations for $0.01 \leqslant \mu \leqslant 100$ show that ε never reaches the value of 40. Thus, considering that the value of $\varepsilon = 40$ corresponds to the relative difference between b_0 (19) and b_0 (20) of only 4×10^{-5} [see equation (37)], we conclude that using only the first 20 equations of the system of (30) is adequate for our purpose here. In what follows, all the results are obtained using b_0 (20).

In Fig. 6, we plot the dimensionless resistance ψ as a function of the dimensionless height h, the conductivity ratio μ being the parameter. We note that $\psi = 1$ when $h = 0$, which is a well known result (see reference [17], for example). Furthermore, as h increases, so does ψ, because a greater h means that there is more material resistance. From Fig. 6, we also observe that for a given h, the resistance ψ and its rate of increase [i.e., $d\psi/dh$) are greater for a larger μ. This is so because, with k_2 fixed, a larger μ means a smaller k_1 and, thus, a larger material resistance of the cylinder Finally, we note that, except for very small values of

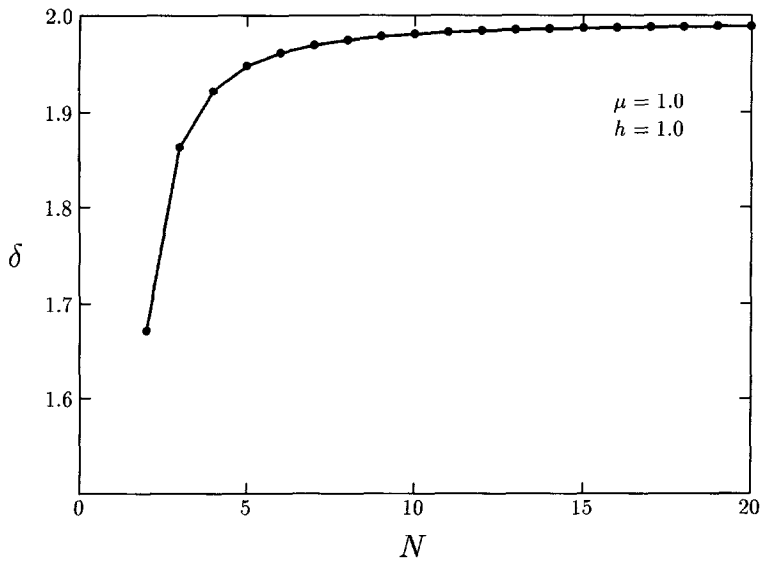

Fig. 3. The quantity δ as a function of N, the number of simultaneous equations used in the calculation of b_0.

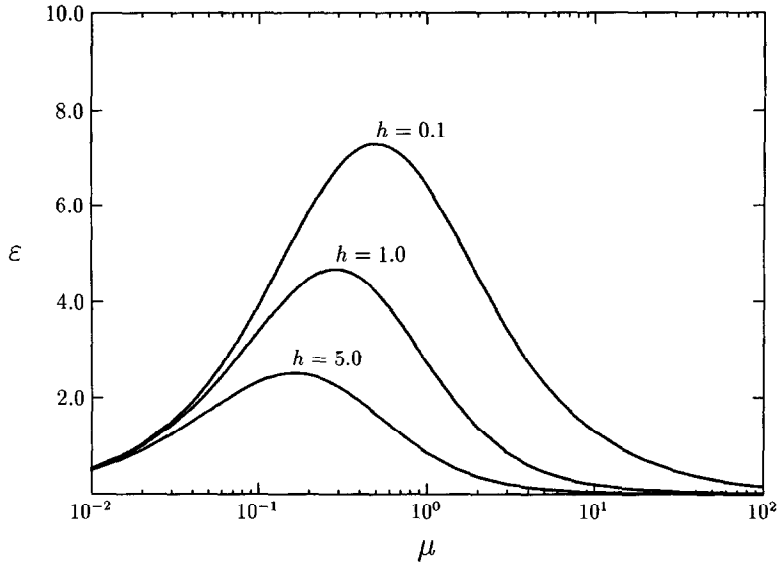

Fig. 4. The quantity ε as a function of the conductivity ratio μ.

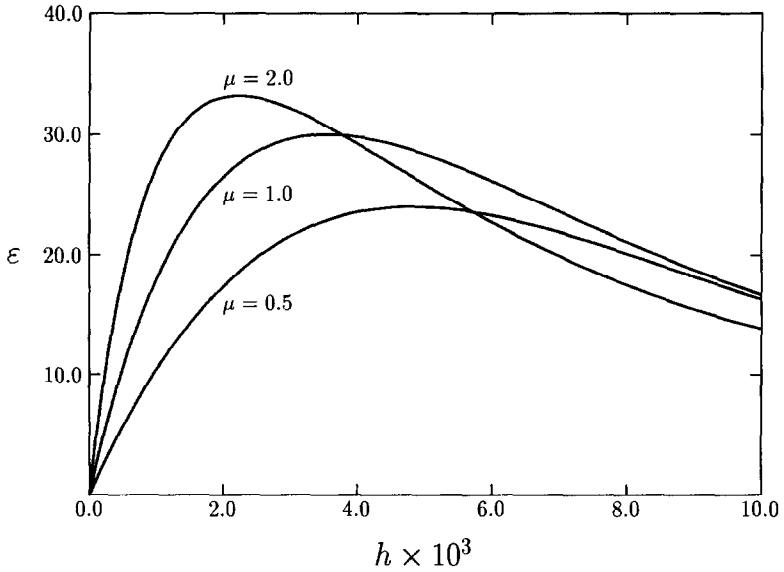

Fig. 5. The quantity ε as a function of the dimensionless height h.

h, the slope $d\psi/dh$ is practically a constant for a given μ.

In Fig. 7, we plot the derivative $\psi' = d\psi/dh$ as a function of h with μ as a parameter. The values of ψ' have been calculated using a fourth-order central difference scheme given by

$$\psi'(h) = \frac{\psi(h-2\Delta h) - 8\psi(h-\Delta h) + 8\psi(h+\Delta h) - \psi(h+2\Delta h)}{12\Delta h} \tag{38}$$

where $\Delta h = 0.025$. From Fig. 7, we see that, for a fixed μ, ψ' approaches its asymptotic value rapidly as we increase the dimensionless height h. This means that except when h is very small, the increase in the thermal resistance is solely due to the increase in the material resistance, which, in turn, is the result of the increased height of the cylinder. To see this quantitatively, we first note that, in dimensionless form, the material resistance of the cylinder against axial heat flow can be derived from equation (14) and is given by

$$\psi_m = \frac{4\mu h}{\pi} \tag{39}$$

$$\varphi_m = \frac{4h}{\pi}. \tag{40}$$

From equation (39), it follows that

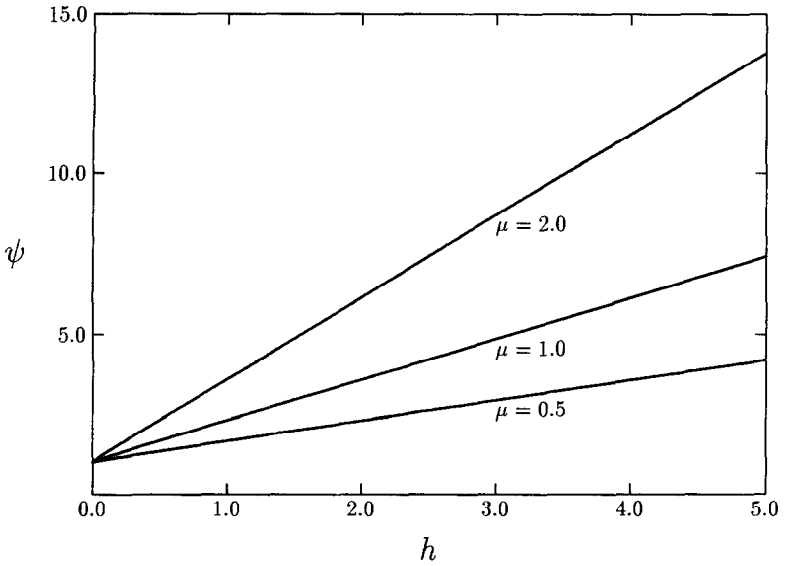

Fig. 6. Thermal resistance ψ as a function of the cylinder's height h.

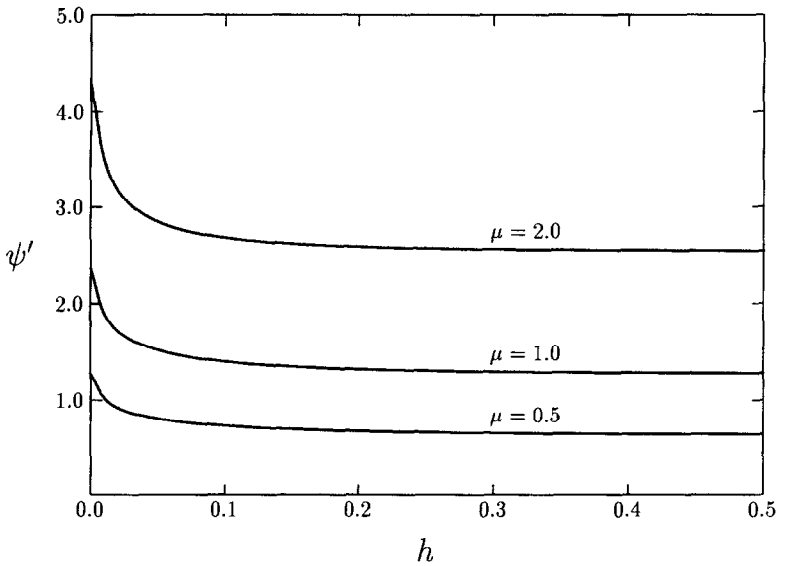

Fig. 7. Derivative of the thermal resistance ψ as a function of the cylinder's height h.

$$\frac{d\psi_m}{dh} = \frac{4\mu}{\pi}. \tag{41}$$

For $\mu = 0.5$, 1.0, 2.0, we read from Fig. 7 that at $h = 0.5$, ψ' is equal to 0.640, 1.277, 2.550, respectively. For the same set of μ, equation (41) yields 0.637, 1.273, 2.546, respectively. From this comparison of Fig. 7 and equation (41), we may conclude that, for practical purposes, ψ' reaches its limiting value when h is increased to $h \sim O(1)$. To summarize what we have observed from Figs. 6 and 7: the resistance ψ increases from $\psi = 1$ when we increase the dimensionless height of the cylinder from $h = 0$. For $h \ll 1$, the increase in ψ results from the increase in both the constriction and material resistances; however, when h has reached the order of 1, further increase in the height of the cylinder results in the increase in the material resistance only, the increase in the constriction resistance being negligible. We shall have a few words on the constriction resistance later.

The behavior of ψ as a function of μ, h being a parameter, is depicted in Fig. 8. We note that for $\mu \to 0$, $\psi = 1$, which is the result for an isothermal contact area on a half space. Physically, a small μ, k_2 being fixed, means that the cylinder is composed of a highly conductive material; consequently, the thermal resistance $\mathscr{R}$ is dominated by the constriction resistance, the material resistance of the cylinder being insignificant.

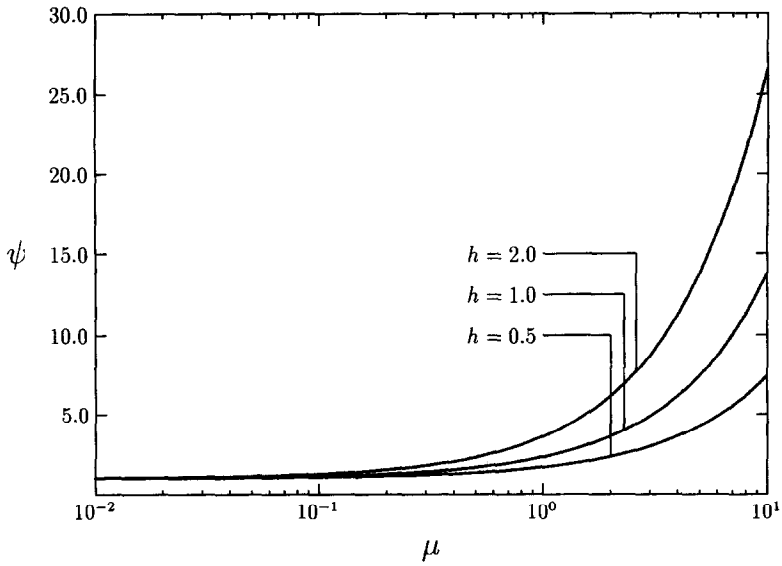

Fig. 8. Thermal resistance ψ as a function of the conductivity ratio μ.

However, when μ increases (i.e., when the material of the cylinder becomes less conductive), the material resistance becomes significant and the thermal resistance increases, as is clearly seen from Fig. 8. When μ is increased beyond a certain value, the material resistance becomes the dominant part of the thermal resistance $\mathscr{R}$, the constriction resistance being insignificant in comparison. In this case, ψ approaches its asymptotic value ψ_m given by equation (39) as $\mu \to \infty$. That is, $\psi \sim \mu$, or, as can be seen from Fig. 8, $\psi \sim e^{\log\mu}$.

To see from a different perspective the dependence of the thermal resistance on the conductivity ratio, let us consider the φ-vs-μ plot of Fig. 9, in which we hold k_1 constant but vary k_2. We observe that as μ increases, the resistance φ decreases; furthermore, when μ becomes sufficiently large, φ approaches asymptotically a limiting value. Physically, this means that as the semi-infinite solid becomes more conductive, the constriction resistance decreases and, since the material resistance is constant, so does the (overall) thermal resistance. When the thermal conductivity of the semi-infinite solid becomes sufficiently large, the constriction resistance becomes insignificant compared to the material resistance. In this case, φ approaches its asymptotic value of φ_m given by equation (40) as $\mu \to \infty$. For $h = 0.5, 1.0, 2.0$, φ_m is equal to 0.634, 1.273, 2.546, respectively. These indeed com-

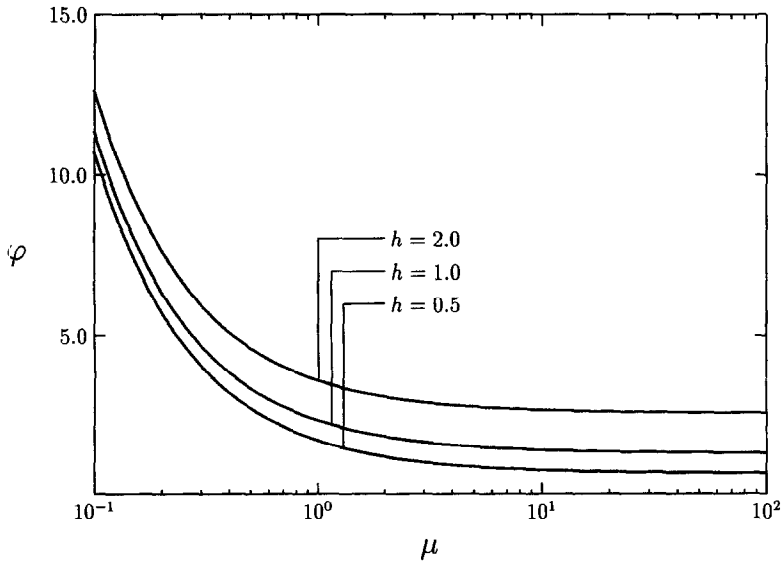

Fig. 9. Thermal resistance φ as a function of the conductivity ratio μ.

pare very favorably with the respective values of 0.647, 1.284, 2.557 at $\mu = 100$ read from Fig 9, considering that φ_m is reached only when μ becomes very large.

From equation (13), we see that the thermal resistance $\mathscr{R}$ consists of two components: the material resistance of the cylinder and the constriction resistance at the interface of the cylinder and the semi-infinite solid. In dimensionless form,

$$\psi = \psi_m + \psi_c \tag{42}$$

where ψ_c is the dimensionless constriction resistance. In Fig. 10, we plot the constriction resistance ψ_c, calculated using equation (42), as a function of the cylinder's height h with the conductivity ratio μ as a parameter. It is seen that for a given conductivity ratio μ, the constriction resistance ψ_c increases with the dimensionless height h and rapidly approaches its asymptotic value. Furthermore, ψ_c reaches it limiting value more rapidly if the conductivity ratio μ is increased. From Fig. 10, we also observe that for a given set of h and k_2, the constriction resistance increases as k_1 decreases. This is hardly unexpected, since a smaller k_1 means a less conductive cylinder and, therefore, a larger constriction resistance. Finally, we note that the increase in the constriction resistance due to a finite height of the cylinder is, for practical purposes, fairly small. Even in the case of $\mu = 100$, for example, the constriction resistance increases by only about 8% from its zero-h value as we increase h to beyond 0.5.

As mentioned earlier in the Introduction, the present study is partly motivated by the applications of BGA in the micro-electronics industry. In connection with the applicability of our study to the BGA joints in micro-electronic packages, Table 1 gives the approximate values of μ for some of the commonly encountered materials. In Table 2, we give the approximate values of the aspect ratio of the cylinder, h, which are applicable to some of the common joint types.

Table 1. The conductivity ratio μ for a 60/40-Pb/Sn cylinder and solid 2 of some common materials

Solid 2	μ
Copper trace	0.19
Silicon	0.4
Al_2O_3	12.5
Epoxy mold compound	75
Out-of-plane PCB	166

Table 2. The aspect ratio h for some common joint types

Joint type	h
OMPAC	≈ 1.5
SBC	≈ 2.9
SCC	8.8

5. CONCLUDING REMARKS

In this paper, we have carried out an analytical study pertaining to the thermal resistance of two semi-infinite solids in contact through a cylindrical joint. Our study is applicable only to the case in which the two solids have the same thermal conductivity. In this case, we can invoke the symmetry of the physical configuration and the uniqueness of the solution for the temperature field, apart from an additive constant, to show that the temperature is uniform throughout

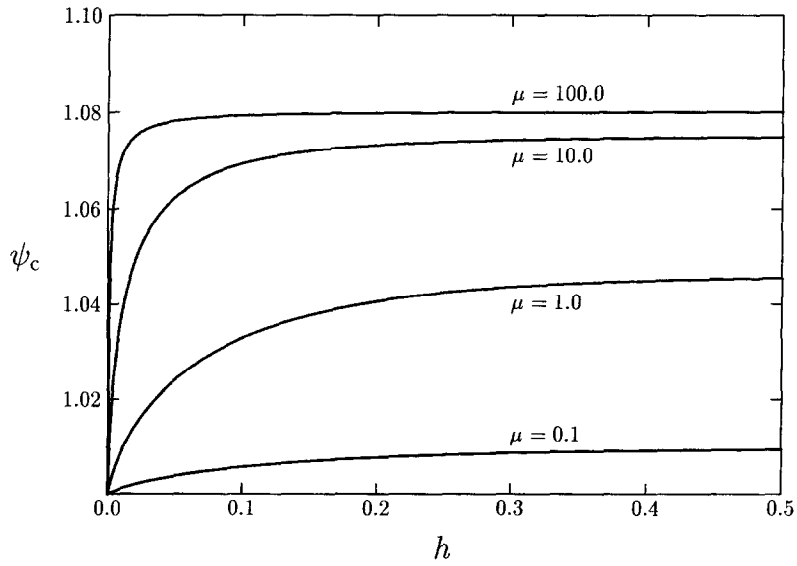

Fig. 10. Thermal constriction resistance ψ_c as a function of the cylinder's height h.

the cross section of the cylinder midway between the two solids. Our problem then reduces to the simpler one which consists of one semi-infinite solid and half of the cylinder. In the more general case in which the two semi-infinite solids have different thermal conductivities, we cannot apply physical symmetry to show that the temperature is uniform at the cross section of the cylinder midway between the two solids. In fact, we expect that the temperature is not uniform there. In a somewhat similar study of two semi-infinite solids with an interstitial body at their interface, Das and Sadhal [19] show that the interface of the two solids is isothermal if and only if geometrical symmetry exists and the two solids have the same thermal conductivity.

Returning to our original problem of two semi-infinite solids of the same thermal conductivity (see Fig. 1), it is easy to show that the thermal resistance $\mathscr{R}_{\text{tot}}$ is given by

$$\mathscr{R}_{\text{tot}} = 2\mathscr{R}. \tag{43}$$

Here, we define $\mathscr{R}_{\text{tot}}$ as

$$\mathscr{R}_{\text{tot}} = \frac{\Delta T_{\text{tot}}}{\dot{Q}} \tag{44}$$

where ΔT_{tot} is the difference between the average surface temperatures of the two semi-infinite solids.

While our study deals with one cylinder only, the results can be applied to the more general case in which the two semi-infinite solids are in contact through a large number of cylinders, provided that any two adjacent cylinders are sufficiently far apart. However, if the cylinders are closely arranged in an array, the error, which is a function of the array type, can become significant, as can be conjectured from the analytical study of Tio and Sadhal [17] for an array of contact areas on a half space. The problem of multiple cylinders is very complicated and, therefore, is not pursued here.

REFERENCES

1. Carslaw, H. S. and Jaeger, J. C., *Conduction of Heat in Solids*. Oxford University Press, London, 1959.
2. Madhusudana, C. V. and Fletcher, L. S., Contact heat transfer—the last decade. *AIAA Journal*, 1986, **24,** 510–523.
3. Snaith, B., Probert, S. D. and O'Callaghan, P. W., Thermal resistances of pressed contacts. *Applied Energy*, 1986, **22,** 31–84.
4. Yovanovich, M. M., Recent developments in thermal contact, gap and joint conductance theories and experiment. *Proceedings of the Eighth International Heat Transfer Conference*, Vol. 1. Hemisphere, Washington, DC, 1986, pp. 35–45.
5. Fletcher, L. S., Recent developments in contact conductance heat transfer. *Journal of Heat Transfer*, 1988, **110,** 1059–1070.
6. Cooper, M. G., Mikic, B. B. and Yovanovich, M. M., Thermal contact conductance. *International Journal of Heat and Mass Transfer*, 1969, **12,** 279–300.
7. Sayles, R. S. and Thomas, T. R., Thermal conductance of a rough elastic contact. *Applied Energy*, 1976, **2,** 249–267.
8. Bush, A. W. and Gibson, R. D., A theoretical investigation of thermal contact conductance. *Applied Energy*, 1979, **5,** 11–22.
9. Majumdar, A. and Tien, C. L., Fractal network model for contact conductance. *Journal of Heat Transfer*, 1991, **113,** 516–525.
10. Hunter, A. and Williams, A., Heat flow across metallic joints—the constriction alleviation factor. *International Journal of Heat and Mass Transfer*, 1969, **12,** 524–526.
11. Gibson, R. D., The contact resistance for a semi-infinite cylinder in a vacuum. *Applied Energy*, 1976, **2,** 57–65.
12. Negus, K. J. and Yovanovich, M. M., Constriction resistance of circular flux tubes with mixed boundary conditions by linear superposition of Neumann solutions. ASME Paper 84-HT-84, 1984.
13. Faltin, C., Exact solution of constriction resistance and temperature field within a homogeneous cylindrical body heated by an isothermal contact spot. *International Communications in Heat and Mass Transfer*, 1985, **12,** 677–686.
14. Gladwell, G. M. L. and Lemczyk, T. F., Thermal constriction resistance of a contact on a circular cylinder with mixed convective boundaries. *Proceedings of the Royal Society of London*, 1988, **A420,** 323–354.
15. Greenwood, J. A., Constriction resistance and the real area of contact. *British Journal of Applied Physics*, 1966, **17,** 1621–1632.
16. Beck, J. V., Effects of multiple sources in the contact conductance theory. *Journal of Heat Transfer*, 1979, **101,** 132–136.
17. Tio, K.-K. and Sadhal, S. S., Thermal constriction resistance: effects of boundary conditions and contact geometries. *International Journal of Heat and Mass Transfer*, 1992, **35,** 1533–1544.
18. Tio, K.-K. and Sadhal, S. S., Analysis of thermal constriction resistance with adiabatic circular gaps. *Journal of Thermophysics and Heat Transfer*, 1991, **5,** 550–559.
19. Das, A. K. and Sadhal, S. S., The effect of interstitial fluid on thermal constriction resistance. *Journal of Heat Transfer*, 1992, **114,** 1045–1048.
20. Das, A. K., Thermal contact conductance—effects of clustering, random distribution and interstitial fluid. Ph.D. thesis, University of Southern California, Los Angeles, 1992.
21. Lau, J. H., A brief introduction to ball grid array technologies. In *Ball Grid Array Technology*, ed. J. H. Lau. McGraw-Hill, New York, 1995, pp. 1–64.
22. Romenesko, B. M., Ball grid array and flip chip technologies: their histories and prospects. *International Journal of Microcircuits and Electronic Packaging*, 1996, **19,** 64–74.
23. Adams, J. A., Inspection of ball grid array assembly. In *Ball Grid Array Technology*, ed. J. H. Lau, McGraw-Hill, New York, 1995, pp. 465–489.
24. Tio, K.-K., Transport problems with spatially periodic mixed interface conditions. Ph.D. thesis, University of Southern California, Los Angeles, 1990.
25. Tio, K.-K. and Sadhal, S. S., Dropwise evaporation: thermal analysis of multidrop systems. *International Journal of Heat and Mass Transfer*, 1992, **35,** 1987–2004.
26. Lebedev, N. N., *Special Functions and Their Applications*. Dover Publications, New York, 1972.
27. Gradshteyn, I. S. and Ryzhik, I. M., *Table of Integrals, Series, and Products*. Academic Press, New York, 1980.
28. Abramowitz, M. and Stegun, I. A., *Handbook of Mathematical Functions*. Dover Publications, New York, 1965.

APPENDIX

To calculate the coefficients C_{nm} [see equation (32)], we need to calculate first the functions $F_m(\lambda_n)$ and $G_m(\lambda_n)$ as well

as the Legendre function of the second kind $Q_m(i0)$ and its derivative $Q'_m(i0)$. Substituting the Legendre polynomial

$$P_m(x) = \sum_{j=0}^{m/2} \frac{(-1)^j(2m-2j)!}{2^m j!(m-j)!(m-2j)!} x^{m-2j}, \quad m = 0, 2, \ldots \tag{A.1}$$

into equation (28), changing the order of integration and summation, and making use of formula (6.567.1) of Gradshteyn and Ryzhik [27], we obtain

$$F_m(\lambda_n) = \frac{1}{2^{m/2}} \sum_{j=0}^{m/2-1} \frac{(-1)^j(2m-2j)!(m/2-j)!}{2^j j!(m-j)!(m-2j)!\lambda_n^{m/2-j+1}} J_{m/2-j+1}(\lambda_n). \tag{A.2}$$

To calculate the function $G_m(\lambda_n)$, we substitute the series expansion

$$J_v(x) = \sum_{j=0}^{\infty} \frac{(-1)^j(x/2)^{v+2j}}{\Gamma(j+1)\Gamma(j+1+v)} \tag{A.3}$$

where Γ denotes the gamma function, into equation (29), interchange the order of integration and summation, and make use of formula (7.132) of Gradshteyn and Ryzhik [27]. Then, after some simple manipulation of the result, we obtain

$$G_m(\lambda_n) = \frac{1 \cdot 3 \cdot 5 \ldots (m-1)}{2 \cdot 4 \cdot 6 \ldots (m)} \left(\frac{\pi}{2\lambda_n}\right)^{1/2} J_{m+1/2}(\lambda_n). \tag{A.4}$$

Equations (A.2) and (A.4) are valid for $m = 2, 4, 6, \ldots$, and all the positive roots $\lambda_1, \lambda_2, \lambda_3, \ldots$, of equation (20). For the special case of $m = 0$,

$$F_0(\lambda_n) = 0, \quad n = 1, 2, \ldots \tag{A.5}$$

$$G_0(\lambda_n) = \left(\frac{\pi}{2\lambda_n}\right)^{1/2} J_{1/2}(\lambda_n), \quad n = 1, 2, \ldots. \tag{A.6}$$

For $\lambda_0 = 0$, we can, with the aid of formula (7.121) of Gradshteyn and Ryzhik [27], derive directly from equation (28) the following expression for $F_m(0)$:

$$F_m(0) = -\frac{P_m(0)}{(m-1)(m+2)}, \quad m = 0, 2, \ldots. \tag{A.7}$$

Making use of the orthogonality of Legendre polynomials, it is straightforward to obtain

$$G_m(0) = \begin{cases} 1, & m = 0 \\ 0, & m = 2, 4, \ldots \end{cases}. \tag{A.8}$$

To calculate the Bessel functions in equations (A.2) and (A.4), we select a sufficiently large v and calculate $J_v(\lambda_n)$ and $J_{v-1}(\lambda_n)$ using the series expansion of equation (A.3). Then, we calculate $J_{v-2}(\lambda_n)$, $J_{v-3}(\lambda_n), \ldots$, successively using the recurrence relation of

$$J_v(\lambda_n) = \frac{2(v+1)}{\lambda_n} J_{v+1}(\lambda_n) - J_{v+2}(\lambda_n). \tag{A.9}$$

Since we use equation (A.9) to calculate the Bessel functions in the direction of decreasing order, this practice is always permissible, as pointed out by Abramowitz and Stegun [28]. The first nineteen positive roots of λ_n, with an accuracy of up to the tenth decimal place, are given in reference [28], and will not be reproduced here.

To calculate $Q_m(i0)$, $m = 2, 4, \ldots$, we start with

$$Q_0(i0) = -i\frac{\pi}{2} \tag{A.10}$$

and use the recurrence relation

$$Q_m(i0) = -\frac{m-1}{m} Q_{m-2}(i0), \quad m = 2, 4, \ldots. \tag{A.11}$$

Similarly, we can use

$$Q'_0(i0) = 1 \tag{A.12}$$

$$Q'_m(i0) = -\frac{m}{m-1} Q'_{m-2}(i0), \quad m = 2, 4, \ldots \tag{A.13}$$

to calculate the first derivatives of $Q'_m(i0)$.